

# Motor-driven Dynamics of Cytoskeletal Filaments in Motility Assays

Shiladitya Banerjee,<sup>1</sup> M. Cristina Marchetti,<sup>2</sup> and Kristian Müller-Nedebock<sup>3</sup>

<sup>1</sup>*Physics Department, Syracuse University, Syracuse, NY 13244, USA*

<sup>2</sup>*Physics Department & Syracuse Biomaterials Institute, Syracuse University, Syracuse, NY 13244, USA*

<sup>3</sup>*Institute of Theoretical Physics/Department of Physics,  
Stellenbosch University, Matieland 7602, South Africa*

(Dated: June 13, 2011)

We model analytically the dynamics of a cytoskeletal filament in a motility assay. The filament is described as rigid rod free to slide in two dimensions. The motor proteins consist of polymeric tails tethered to the plane and modeled as linear springs and motor heads that bind to the filament. As in related models of rigid and soft two-state motors, the binding/unbinding dynamics of the motor heads and the dependence of the transition rates on the load exerted by the motor tails play a crucial role in controlling the filament's dynamics. Our work shows that the filament effectively behaves as a self-propelled rod at long times, but with non-Markovian noise sources arising from the coupling to the motor binding/unbinding dynamics. The effective propulsion force of the filament and the active renormalization of the various friction and diffusion constants are calculated in terms of microscopic motor and filament parameters. These quantities could be probed by optical force microscopy.

There has recently been renewed interest in motility assays where semiflexible actin filaments are driven to slide over a “bed” of myosin molecular motors. Recent experiments at high actin density have revealed that the collective behavior of this simple active system is very rich, with propagating density waves and large scale-swirling motion [1, 2], not unlike those observed in dense bacterial suspensions [3]. In an actin motility assay the polymeric tails of myosin motor proteins are anchored to a surface, while their heads can bind to actin filaments [4]. Once bound, the motor head exerts forces and drives the filament's motion. This system provides possibly the simplest realization of an active system that allows detailed semi-microscopic modeling.

Stochastic models of the collective action of motor proteins on cytoskeletal filaments in *one dimension* have been considered before by several authors, with emphasis on the acto-myosin system in muscles and on the mitotic spindle [5]. When working against an elastic load, the motor assemblies have been shown to drive periodic spontaneous activity in the form of oscillatory instabilities, which in turn have been observed ubiquitously in a variety of biological systems [6–10]. These instabilities arise in the model from the collective action of the motors and the breaking of detailed balance in their dynamics and manifest themselves as a negative effective friction of the filament. When free to slide under the action of an external force, the filament can exhibit bistability that manifests itself as hysteresis in the force velocity-curve [11, 12]. A large body of earlier work has modeled the motors as rigid two-state systems attached to a backbone and bound by the periodic potential exerted by the filament on the motor head [6, 11, 13]. In a second class of models the motors have been modeled as flexible springs [14, 15]. The motor heads bind to the filament and unbind at a load-dependent rate. In this case the dynamic instability arises from the dependence of the unbinding rate on the tension exerted by springs [16–18].

Recent work by Guérin et al. [19] has generalized the two-state model by taking into account the flexibility of the motors, showing that both models can be obtained in a unified manner for different values of a parameter that compares the stiffness of the motors to the stiffness of the periodic potential provided by the filament.

In this paper we consider a model of a rigid filament free to slide in *two dimensions* under the driving action of motor proteins uniformly tethered to a two-dimensional plane. The model considered is a modification of the “crossbridge” model first introduced by Huxley in 1957 to describe motor-induced contractile behavior of muscle fibers [20]. The motor proteins' polymeric tails are modeled as linear springs that pull back on the bound motor heads. After attachment, the motor heads slide along the filament at a velocity that depends on the load exerted by the flexible motor tails. The sliding and subsequent detachment play the role of the motor's power stroke. The binding/unbinding dynamics of the motor heads and the dependence of the transition rates on the load exerted by the motor tails play a crucial role in controlling the dynamics of the filament, effectively yielding non-Markovian noise sources on the filament. Related models have been studied numerically [14, 15, 21]. The results presented here are obtained by generalizing to two dimensions the mean field approximation for the motor dynamics described for instance in Ref. [7]. The mean-field theory neglects convective nonlinearities in the equation for the probability of bound motors and correlations in the motors on/off dynamics, but it is expected to be adequate on time scales large compared to that of the motor on/off dynamics and for a large number of motors. This is supported by the results of [11] for a model of rigid two-state motors.

We begin by revisiting the one-dimensional problem. We discuss the steady-state response of the filament to an external force and present new results on the dynamics of fluctuations about the sliding steady state. The

force-velocity curve is evaluated analytically and exhibits bistability and hysteresis, as obtained in Ref. [11] for a rigid two-state motor model. A new result is an expression for the effective propulsion force on the filament due to the motors in terms of physical parameters characterizing the motor proteins. Next, we analyze the fluctuations about the steady state by evaluating the mean-square displacement of the filament. We show that the coupling to the motor binding/unbinding dynamics yields non-Markovian noise sources with time correlations controlled by the duration of the motors' binding/unbinding cycle. Since the filament has a finite motor-induced velocity even in the absence of applied force, the mean-square displacement is ballistic at long time. The fluctuations of displacement about this sliding state are, however, diffusive at long times with an enhanced diffusion constant. This enhancement is controlled by the dependence of the motors' unbinding rate on the load exerted on the bound motors' heads by the tethered tails and vanishes for unloaded motors.

We then consider the case of a filament in two dimensions, to analyze the effect of the coupling of translational and rotational degrees of freedom in controlling the dynamics. At steady state, motors yield an effective propulsion force along the long axis of the filament, as in one dimension, but no effective torque. This is in contrast to phenomenological models considered in the literature [22] that have considered the dynamics of active rod-like particles in the presence of both effective internal forces and torques. As a result, in the steady-state the filament slides along its long axis and the dynamics in this direction is essentially one dimensional, with a motor-induced negative friction instability and bistability and hysteresis in the response to an external force. Motors do enhance both the transverse and the rotational friction coefficients of the filament. The enhancement of rotational friction could be probed by measuring the response to an external torque. Since the finite motor-induced propulsion is along the filament axis, whose direction is in turn randomized by rotational diffusion, the mean velocity of the filament is zero in the absence of external force, unlike in the one-dimensional case. The mean square displacement is therefore diffusive at long times, with behavior controlled by the interplay of non-Markovian effects due to the coupling to motor dynamics with coupled translational and rotational diffusions. The filament performs a persistent random walk that consists of ballistic excursions at the motor-induced propulsion speed, randomized by both rotational diffusion and the motor binding/unbinding dynamics. The crossover to the long-time diffusive behavior is controlled by the interplay of motor-renormalized diffusion rate and duration of the motor binding/unbinding cycle. The effective diffusion constant is calculated in terms of microscopic motor and filament parameters. Its dependence on activity, as characterized by the rate of ATP consumption, could be probed in actin assays.

Finally, our work provides a microscopic justification

of a simple model used in the literature [23] that describes a cytoskeletal filament interacting with motor proteins tethered to a plane as a "self-propelled" rod, although it also shows that the effective noise is rendered non-Markovian by the coupling to the motors' binding/unbinding dynamics. It also provides microscopic expressions for the self-propulsion force and the various friction coefficients in terms of motor and filament parameters and shows that this effective model fails beyond a critical value of motor activity, where the effective friction changes sign and the filament exhibits bistability and hysteresis.

## I. THE MODEL

In our model the motor proteins are described as composed of polymeric tails attached permanently to a two-dimensional fixed substrate and motor heads that can bind reversibly to the filament. Once bound, a motor head moves along the filament thereby stretching the tail. This gives rise to a load force on the motor head and on the filament. Eventually excessive load leads to detachment of the motor head.

### A. Filament dynamics

The actin filament is modeled as a rigid polar rod of length  $L$  that can slide in two dimensions. It is described by the position  $\mathbf{r}$  of its center of mass and a unit vector  $\hat{\mathbf{u}} = (\cos(\theta), \sin(\theta))$  directed along the rod's long axis *away* from the polar direction of the rod, which is in turn defined as the direction of motion of bound motors. In other words, bound motors move along the rod in the direction  $-\hat{\mathbf{u}}$ . In contrast to most previous work [6, 7, 13, 19], and given our interest in modeling actin motility assays, we assume the substrate is fixed and consider the dynamics of the filament. Our goal is to understand the role of the cooperative driving by motors in controlling the coupled rotational and translational dynamics of the rod.

The dynamics of the filament is described by coupled equations for the translational and orientational degrees of freedom, given by

$$\underline{\zeta} \cdot \partial_t \mathbf{r} = \mathbf{F}_a + \mathbf{F}_{\text{ext}} + \boldsymbol{\eta}(t), \quad (1a)$$

$$\zeta_\theta \partial_t \theta = T_a + T_{\text{ext}} + \eta_\theta(t). \quad (1b)$$

Here we have grouped the forces and torques into the effects due to the motors, *i.e.* the activity,  $\mathbf{F}_a$  and  $T_a$ , external forces and torques  $\mathbf{F}_{\text{ext}}$  and  $T_{\text{ext}}$  and the stochastic noise not due to motors. The friction tensor is given by  $\underline{\zeta} = \zeta_\parallel \hat{\mathbf{u}}\hat{\mathbf{u}} + \zeta_\perp (\underline{\delta} - \hat{\mathbf{u}}\hat{\mathbf{u}})$  with  $\zeta_\parallel$  and  $\zeta_\perp$  the friction coefficients for motion longitudinal and transverse to the long direction of the rod, and  $\zeta_\theta$  is the rotational friction coefficient. For the case of a long, thin rod of interest here,  $\zeta_\parallel = \zeta_\perp/2$ . The random force  $\boldsymbol{\eta}(t)$  and

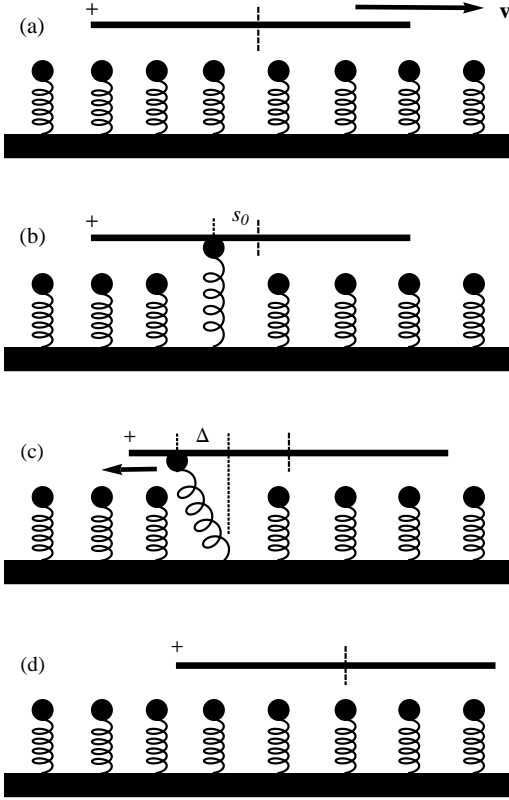


FIG. 1: The figure shows the four steps of a motor cycle. In (a) a filament is sliding with velocity  $v$  over a uniform density of unbound motors with tails tethered to the substrate. In (b) a motor attaches to the filament at a position  $s_0$  from the filament's mid-point. The stretch of the motor tails at the time of attachment is neglected. In (c) the motor has walked towards the polar head of the filament, stretching the tails by an amount  $\Delta$ . Finally, in (d) the bound motor detaches and relaxes instantaneously to its unstretched state. The filament has undergone a net displacement in the direction opposite to that of motor motion.

random torque  $\eta_\theta(t)$  describe noise in the system, including nonthermal noise sources. For simplicity we assume that both  $\boldsymbol{\eta}(t)$  and  $\eta_\theta(t)$  describe Gaussian white noise, with zero mean and correlations  $\langle \eta_i(t) \eta_j(t') \rangle = 2B_{ij} \delta(t - t')$  and  $\langle \eta_\theta(t) \eta_\theta(t') \rangle = 2B_\theta \delta(t - t')$ , where  $B_{ij} = B_{\parallel} \hat{u}_i \hat{u}_j + B_{\perp} (\delta_{ij} - \hat{u}_i \hat{u}_j)$ .

### B. Individual motor dynamics

We model the interaction cycle of an individual motor protein with the filament as shown in Fig. 1 for a one-dimensional system. The tail of a specific motor is fixed at position  $\mathbf{x}_t$  in the plane. At a time  $t_0$  the head of this motor attaches to a point on the filament. The position of the motor head at the time of attachment is  $\mathbf{x}_h(t_0) = \mathbf{r}(t_0) + s_0 \hat{\mathbf{u}}(t_0)$ , where  $\mathbf{r}(t_0)$  and  $\hat{\mathbf{u}}(t_0)$  denote the position of the center of the filament and its orientation  $t = t_0$

and  $s_0 \in [-L/2, L/2]$  parametrizes the distance of the point of attachment from the center of the filament (cf. Fig. 1(b)). We assume that motor proteins will attach to parts of the filament which are within a distance of the order of the size of the motor protein. The stretch of the motor tail at the time of attachment is then of order of the motor size and will be neglected, *i.e.*  $\mathbf{x}_h(t_0) - \mathbf{x}_t = 0$ , or motors attach to the part of the filament directly overhead without any initial stretch.

For  $t > t_0$  the motor head remains attached to the filament and walks along it towards the polar head ( $-\hat{\mathbf{u}}$  direction) until detachment. The tails, modeled as a linear spring of force constant  $k$ , exert a load  $\mathbf{f} = -k\Delta(t, \tau; s_0)$  on the head, where  $\Delta(t, \tau; s_0) = \mathbf{x}_h(t) - \mathbf{x}_t$  is the stretch at time  $t$  of a motor protein that has been attached for a time  $\tau$ , *i.e.*  $t = t_0 + \tau$  (cf. Fig. 1(c)). Since we assume  $\Delta(t_0) = 0$ , we can also write

$$\Delta(t, \tau; s_0) = \mathbf{r}(t) - \mathbf{r}(t - \tau) + \sigma(t, \tau) \hat{\mathbf{u}}(t) + s_0 [\hat{\mathbf{u}}(t) - \hat{\mathbf{u}}(t - \tau)], \quad (2)$$

where  $\sigma(t, \tau) = s(t) - s(t - \tau)$  is the distance traveled along the filament at time  $t$  by a motor head that has been attached for a time  $\tau$ , measured from the initial attachment position,  $s_0$ . The kinematic constraint imposed by the condition of attachment requires

$$\partial_t \Delta(t, \tau; s_0) = \mathbf{v}(t) - \mathbf{v}(t - \tau) + \hat{\mathbf{u}}(t) [v_m(t) - v_m(t - \tau)] + \boldsymbol{\Omega}(t) \sigma(t, \tau) + s_0 [\boldsymbol{\Omega}(t) - \boldsymbol{\Omega}(t - \tau)], \quad (3)$$

where  $\boldsymbol{\Omega}(t) = \partial_t \hat{\mathbf{u}}(t) = \dot{\theta} \hat{\mathbf{n}}(t)$  is the angular velocity of the rod and  $v_m(t) = \partial_t s(t)$  the velocity of the motor head along the filament. We have introduced a unit vector  $\hat{\mathbf{n}} = \hat{\mathbf{z}} \times \hat{\mathbf{u}}$  normal to the long axis of the filament. Then  $(\hat{\mathbf{z}}, \hat{\mathbf{u}}, \hat{\mathbf{n}})$  defines a right-handed coordinate system with in-plane axes longitudinal and transverse to the filament. We note that Eq. (3) can also be written as

$$\partial_t \Delta(t, \tau; s_0) + \partial_\tau \Delta(t, \tau; s_0) = \mathbf{v}(t) + v_m(t) \hat{\mathbf{u}}(t) + \boldsymbol{\Omega}(t) \sigma(t, \tau) + s_0 \boldsymbol{\Omega}(t). \quad (4)$$

While the motor remains bound, the dynamics of the motor head along the filament is described by an overdamped equation of motion

$$\zeta_m \dot{s}(t) = -f_s + \hat{\mathbf{u}} \cdot \mathbf{f} \quad (5)$$

where  $f_s > 0$  is the stall force, defined as the force where the velocity  $v_m = \dot{s}$  of the loaded motor vanishes. Since motors move in the  $-\hat{\mathbf{u}}$  direction, generally  $v_m = \dot{s} < 0$ . Letting  $f_{\parallel} = \hat{\mathbf{u}} \cdot \mathbf{f} = -k\Delta_{\parallel}$ , Eq. (5) can also be written as

$$v_m(t) = -v_0 \left( 1 - \frac{f_{\parallel}(\Delta_{\parallel})}{f_s} \right), \quad (6)$$

where  $v_0 = f_s / \zeta_m \sim \Delta\mu > 0$  is the load-free stepping velocity, with  $\Delta\mu$  the rate of ATP consumption. The motor velocity is shown in Fig. (2) as a function of the load  $f_{\parallel}$ .

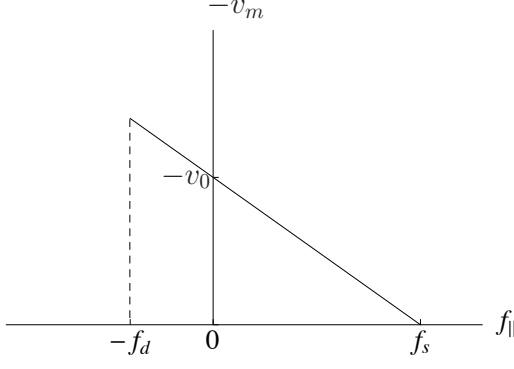


FIG. 2: The velocity  $-v_m$  of a loaded motor head as a function of the load  $f_{\parallel} = \hat{\mathbf{u}} \cdot \mathbf{\Delta}$ . The figure shows the stall force  $f_s$  where  $v_m = 0$  and the detachment force  $-f_d$ .

The motor head velocity also vanishes for  $f_{\parallel} < -f_d$ , when the motor detaches. The linear force-velocity relation for an individual motor is consistent with experiments on single kinesin molecules [24].

The active force and torque on the filament due to an individual bound motor can then be expressed in terms of these quantities as

$$\mathbf{f}_a(t, \tau; s_0) = -k\mathbf{\Delta}(t, \tau; s_0), \quad (7a)$$

$$\tau_a(t, \tau; s_0) = -\hat{\mathbf{z}} \cdot [(s_0 + \sigma(t, \tau))\hat{\mathbf{u}}(t) \times k\mathbf{\Delta}(t, \tau; s_0)]. \quad (7b)$$

Finally, after traveling along the filament for a time  $\tau_{\text{detach}}$ , the motor head detaches and the head position relaxes instantaneously back to the fixed position  $\mathbf{x}_t$  of the tail.

We note that we shall not be considering the possibility of direct interactions of motors with each other. We have also not considered stochastic aspects of the motor motion along the filament (Eq. (5)).

### C. Motor binding and unbinding

Next we need to describe the stochastic binding/unbinding dynamics of the motor heads. We assume the motor tails are attached to the substrate with a homogeneous surface density  $\rho_m$ , such that for a rod of length  $L$  and width  $b$  a maximum of  $N = \rho_m Lb$  motors can be bound at any given time. Following Guérin et al. [19], we denote by  $\mathcal{P}_b(t, \tau; s_0)$  the probability that a motor head that has attached at  $s_0$  at a time  $t_0$ , has remained attached for a duration  $\tau$  at time  $t$ . For simplicity in the following we assume that the probability that a motor attaches at any point along the filament is uniform, i.e.,  $\mathcal{P}_b(t, \tau; s_0) = \frac{1}{L} P_b(t, \tau)$ . We further assume that when motors unbind they relax instantaneously to the unstretched state. The time evolution of the binding

probability is then given by

$$\partial_t P_b(t, \tau) + \partial_\tau P_b(t, \tau) = -\langle \omega_u(\mathbf{\Delta}(\tau)) \rangle_{s_0} P_b(t, \tau) + \omega_b \delta(\tau) p_u(t), \quad (8)$$

where  $p_u(t)$  is the probability that a motor be unbound at time  $t$ . The probability distribution is normalized according to

$$\int_0^\infty d\tau \int_{-L/2}^{L/2} ds_0 \mathcal{P}_b(t, \tau; s_0) + p_u(t) = 1. \quad (9)$$

In Eq. (8),  $\omega_u(\mathbf{\Delta}(\tau))$  and  $\omega_b$  are the rates at which a motor head with tails stretched by an amount  $\mathbf{\Delta}(t, \tau)$  unbinds from and binds to the filament, respectively. The binding rate  $\omega_b$  will be assumed to be constant. In contrast, the unbinding rate  $\omega_u$  is a strong function of the stretch of the motor tails, that has to be obtained by solving Eq. (4), with initial condition  $\mathbf{\Delta}(t=0, \tau) = 0$ . We will see below that the nonlinear dependence of the unbinding rate plays an important role in controlling the filament dynamics. In two dimensions the unbinding rate  $\omega_u$  also depends on the initial attachment point  $s_0$  along the filament. To be consistent with our ansatz that the probability that the motor attaches at any point along the filament is uniform, we have replaced the rate in Eq. (8) with its mean value  $\langle \omega_u \rangle_{s_0}$ , where  $\langle \dots \rangle_{s_0} = \int_{-L/2}^{L/2} \frac{ds}{L} \dots$  denotes an average over the initial attachment points.

The unbinding rate is controlled by the work done by the force (load) acting on the motor head, which in turn is a linear function of the stretch  $\mathbf{\Delta}$ . A form that has been used extensively in the literature for one-dimensional models is an exponential,  $\omega_u = \omega_0 e^{\alpha|\mathbf{\Delta}|}$ , where  $\omega_0$  is the unbinding rate of an unloaded motor and  $\alpha$  is a characteristic length scale that control the maximum stretch of the tails above which the motor unbinds [34]. The exponential form represents an approximation for the result of a detailed calculation of the average time that a motor moving along a polar filament spends attached to the filament as a function of a tangentially applied load [25] and is consistent with experiments on kinesin [26]. This form can easily be generalized to the case of a filament sliding in two dimensions where the motor load had both components tangential and transverse to the filament. It is, however, shown in the Appendix that within the mean-field approximation used below the exponential form yields a steady-state stretch  $\mathbf{\Delta}$  that saturates to a finite value at large velocity  $v$  of the filament. This is unphysical as it does not incorporate the cutoff described by the detachment force  $f_d$  in Fig. 2. For this reason in the mean-field treatment described below we use a parabolic form for the unbinding rate as a function of stretch,

$$\omega_u(\mathbf{\Delta}) = \omega_0 [1 + \alpha^2 |\mathbf{\Delta}|^2], \quad (10)$$

where for simplicity we have assumed an isotropic dependence on the magnitude of the stretch in terms of a

single length scale,  $\alpha^{-1}$ . An explicit comparison of the two expressions for the unbinding rates is given in the Appendix.

The total active force and torque on the filament averaged over the original positions and the times of attachment can be written as

$$\mathbf{F}_a(t) = -Nk \int_0^\infty d\tau \langle P_b(t, \tau) \mathbf{\Delta}(t, \tau; s_0) \rangle_{s_0}, \quad (11a)$$

$$T_a(t) = -Nk \int_0^\infty d\tau \langle P_b(t, \tau) \hat{\mathbf{z}} \cdot [(s_0 + \sigma(t, \tau)) \hat{\mathbf{u}}(t) \times \mathbf{\Delta}(t, \tau; s_0)] \rangle_{s_0}. \quad (11b)$$

## II. MEAN FIELD APPROXIMATION

To proceed, we introduce several approximations for the motor dynamics. First, we restrict ourselves to the dynamics on times scales large compared to the attachment time  $\tau$  of individual motors. For  $t \gg \tau$  we approximate

$$\sigma(t, \tau) \simeq v_m(t)\tau, \quad (12a)$$

$$\mathbf{\Delta}(t, \tau; s_0) \simeq [\mathbf{v}(t) + v_m(t)\hat{\mathbf{u}}(t) + s_0\mathbf{\Omega}(t)]\tau. \quad (12b)$$

This approximation becomes exact for steady states where the filament and motor velocities are independent of time. We also stress that in Eqs. (12a) and (12b)  $\sigma$  and  $\mathbf{\Delta}$  are still nonlinear functions of  $\tau$  due to the dependence of  $v_m$  on the load force.

Secondly, we recall that we have assumed that the attachment positions  $s_0$  are uniformly distributed along the filament and can be treated as independent of the residence times  $\tau$ . Finally, we make a mean field assumption on the probability distribution of attachment times, which is chosen of the form  $P(t, \tau) = \delta(\tau - \tau_{\text{MF}})p_b(t)$ , with  $p_b(t)$  the probability that a motor be attached at

time  $t$  regardless of the its attachment time. The mean-field value of the attachment time is determined by requiring

$$\tau_{\text{MF}} = [\langle \omega_u (\Delta(\tau_{\text{MF}})) \rangle_{s_0}]^{-1}. \quad (13)$$

In previous literature a similar mean field assumption has been stated in terms of the stretch,  $\mathbf{\Delta}$  [7, 8]. In the present problem, however, where filaments can slide in two dimensions, it is necessary to restate the mean-field theory in terms of the residence time  $\tau$  as the active forces and torques depend on both the stretch  $\mathbf{\Delta}$  of the motor tails and the distance  $\sigma$  traveled by a bound motor head along the filament. These two quantities are in turn both controlled by a single stochastic variable, identified with the residence time  $\tau$ . The rate of change of the probability  $p_b(t)$  that a motor be bound at time  $t$  is then described by the equation

$$\partial_t p_b(t) = -\tau_{\text{MF}}^{-1} p_b(t) + \omega_b [1 - p_b(t)], \quad (14)$$

The mean field active force and torque due to the motors are then given by

$$\mathbf{F}_a^{\text{MF}} = -kN \langle \mathbf{\Delta}(t, \tau_{\text{MF}}; s_0) p_b(t) \rangle_{s_0}, \quad (15)$$

$$T_a^{\text{MF}} = -kN \langle p_b(t) \hat{\mathbf{z}} \cdot [(s_0 + \sigma(t, \tau_{\text{MF}})) \hat{\mathbf{u}}(t) \times \mathbf{\Delta}(t, \tau_{\text{MF}}; s_0)] \rangle_{s_0}. \quad (16)$$

In the following we will work in the mean-field approximation and remove the label MF from the various quantities.

## III. ACTIVE FILAMENT SLIDING IN ONE DIMENSION

We first consider the simplest theoretical realization of a motility assay experiment, where the actin filament is sliding over a one dimensional track of tethered motor

proteins. A closely related model, where the filament is elastically coupled to a network, has been used extensively in the literature to study the onset of spontaneous oscillations arising from the collective action of the bound motors [6, 7, 11]. Previous studies of freely sliding filaments, as appropriate for the modeling of motility assays, have also been carried out both analytically and numerically [18]. Our work contains some new results on the response to an external force of a filament free to slide under the action of active crosslinkers and also on the filament fluctuations.

Parameters	Myosin-II	Kinesin
$\ell_0$	$\sim 2$ nm	$\sim 8$ nm
$\delta_s$	$\sim 1$ nm	$\sim 25$ nm
$\epsilon$	$\sim 2$	$\sim 0.32$

TABLE I: Typical values of the length scales  $\ell_0 = v_0/\omega_0$  and  $\delta_s = f_s/k$  introduced in the text and the ratio  $\epsilon$  for myosin II and kinesin. The parameters are taken from Refs. [27] and [14].

The Langevin equation for the center of mass coordinate  $x$  of the filament is given by

$$\zeta \dot{x} = F_a(t) + F_{\text{ext}} + \eta(t), \quad (17)$$

where  $\dot{x}$  is the center-of-mass velocity of the filament and the mean-field active force is given by

$$F_a^{\text{MF}}(t) = -kNp_b(t)\Delta(\dot{x}, \tau). \quad (18)$$

In one dimension the dependence on  $s_0$  drops out and Eq. (12b) simply gives  $\Delta \simeq (\dot{x} + v_m)\tau$ . Substituting Eq. (6) for  $v_m$ , we can solve for  $\Delta$  as a function of  $\dot{x}$  and  $\tau$ ,

$$\Delta(\dot{x}, \tau) = \frac{(\dot{x} - v_0)/\omega_0}{\tilde{\tau}^{-1} + \epsilon}, \quad (19)$$

and Eq. (13) for the mean attachment time becomes

$$\tilde{\tau}^{-1}(\dot{x}) = 1 + \frac{(\dot{x} - v_0)^2 \alpha^2}{[\tilde{\tau}^{-1}(\dot{x}) + \epsilon]^2 \omega_0^2}, \quad (20)$$

where  $\tilde{\tau} = \omega_0 \tau$  and  $\epsilon = kv_0/f_s \omega_0$ . The parameter  $\epsilon$  is the ratio of the length  $\ell_0 = v_0/\omega_0$  traveled by an unloaded motor that remains attached for a time  $\omega_0^{-1}$  to the stretch  $\delta_s = f_s/k$  of the motor tails at the stall force,  $f_s$ . Typical values for these length scales and the parameter  $\epsilon$  are given in Table I.

It is convenient to rewrite the mean residence time  $\tilde{\tau}$  as

$$\tilde{\tau}^{-1} = 1 + \frac{(u - 1)^2 \nu^2}{[\tilde{\tau}^{-1} + \epsilon]^2}, \quad (21)$$

where  $u = \dot{x}/v_0$  and we have introduced a dimensionless parameter  $\nu = \ell \alpha$  that controls the dependence of the unbinding rate on the load exerted on the bound heads by the stretched motor tails, with

$$\frac{1}{\ell} = \frac{1}{\ell_0} + \frac{1}{\delta_s} \quad (22)$$

the geometric mean of the two length scales introduced earlier. For stiff motors, with  $\epsilon \gg 1$  or  $\ell_0 \gg \delta_s$ ,  $\ell \sim \delta_s$ , while for floppy, easy to stretch motors, corresponding to  $\epsilon \ll 1$  or  $\ell_0 \ll \delta_s$ ,  $\ell \sim \ell_0$ . Setting  $\nu = 0$  corresponds to neglecting the load dependence of the unbinding rate. The exact solution to Eq. (21) for the mean residence time  $\tilde{\tau}(\dot{x})$  as a function of the filament velocity can be determined and is discussed in the Appendix. Clearly  $\tau$  has a maximum value at  $\dot{x} = v_0$ , where  $\tau = \omega_0^{-1}$  and decays rapidly as  $|\dot{x} - v_0|$  grows.

## A. Steady State and its Stability

We begin by characterizing the steady state dynamics of the filament in the absence of noise. Incorporating for generality an external force  $F_{\text{ext}}$ , the steady state velocity  $v$  of the filament is obtained from the solution of the nonlinear equation

$$\zeta v = F_{\text{ext}} + F_a(v) \quad (23)$$

where  $F_a(v) = -kNp_{bs}(v)\Delta(v)$ . The steady state stretch  $\Delta(v)$  is given by Eq. (19) with  $\dot{x} = v$  and

$$p_{bs}(v) = \frac{\omega_b \tau(v)}{1 + \tau(v)\omega_b}, \quad (24)$$

with  $\tau(v)$  given by Eq. (21) for  $\dot{x} = v$ . To gain some insight in the behavior of the system, we expand the active force as  $F_a(v) \simeq F_p + \left(\frac{\partial F_a}{\partial v}\right)_{v=0} v + \mathcal{O}(v^2)$ , with  $F_p = F_a(v = 0)$ . Retaining only terms linear in  $v$  this gives a steady state force/velocity relation of the form

$$(\zeta + \zeta_a)v = F_{\text{ext}} + F_p \quad (25)$$

with a filament “propulsion” force  $F_p$

$$F_p = \frac{Np_{bs0}k\ell_0}{\epsilon + \tilde{\tau}_0^{-1}}, \quad (26)$$

where  $p_{bs0} = r/[r + (1-r)\tilde{\tau}_0^{-1}]$ , with  $r = \omega_b/(\omega_0 + \omega_b)$  the duty ratio, and  $\tilde{\tau}_0 = \tilde{\tau}(v = 0)$ . The active contribution  $\zeta_a = -\left(\frac{\partial F_a}{\partial v}\right)_{v=0}$  to the friction is given by

$$\zeta_a = Np_{bs0} \frac{k|\Delta_0|}{v_0} \left[ 1 - \left( \frac{|\Delta_0|}{\ell_0} + p_{bs0} \frac{1-r}{r} \right) \frac{2\alpha^2 \Delta_0^2 \ell_0}{\ell_0 + 2\alpha^2 |\Delta_0|^3} \right] \quad (27)$$

where  $\Delta_0 = \Delta(v = 0) = -\ell_0/(\tilde{\tau}_0^{-1} + \epsilon)$ . In the absence of external force, the filament will slide at a velocity

$$v_s = F_p/(\zeta + \zeta_a) \quad (28)$$

due to the action of the motor proteins. This motion is in the polar direction of the filament and opposite to the direction of motion of bound motors along the filament. Phenomenological models of motility assays have described the actin filaments as “self-propelled” Brownian rods. Our model yields a microscopic calculation of such a “self-propulsion” force  $F_p$  in terms of microscopic parameters characterizing the motor proteins. We note that  $-F_p$  can also be interpreted as the “stall force” of the filament, *i.e.* the value of  $F_{\text{ext}}$  required to yield  $v = 0$ . This is a quantity that may be experimentally accessible using optical force microscopy.

If we neglect the load dependence of the unbinding rate by letting  $\nu = 0$ , the mean number of bound motors is simply  $Nr$  and  $F_p^0 = Nr k \ell$ , with  $\ell$  given by Eq. (22). In this limit the sliding velocity  $v_s^0$  in the absence of external force can be written as

$$v_s^0 = \frac{v_0}{1 + \zeta/\zeta_a^0}. \quad (29)$$

where the active friction  $\zeta_a^0 = Nrkl/v_0 > 0$  is always positive. The sliding velocity vanishes when  $v_0 \rightarrow 0$  and it saturates to its largest value  $v_0$  when the number  $Nr$  of bound motors becomes very large and  $\zeta_a^0 \gg \zeta$ . The behavior is controlled by the parameter  $\epsilon$ . If the motors are easy to stretch, i.e.,  $\epsilon \ll 1$ , then the propulsion force is determined entirely by the elastic forces exerted by these weak bound motors, with  $F_p^0 \simeq Nrkl_0$ . On the other hand stiff motors, with  $\epsilon \gg 1$ , stall before detaching. The propulsion force is then controlled by the motor stall force, with  $F_p^0 \simeq Nrf_s$ .

The load-dependence of the unbinding rate changes qualitatively the behavior of the system. In particular, the net friction  $\zeta + \zeta_a$  can become negative, rendering the steady state unstable. This instability was already noted in Ref. [11] for a two-state model of active linkers and in Ref. [19] for a two state “soft” motor model. The full nonlinear force-velocity curves are shown in Fig. 3 for various values of the motor stiffness  $k$ , for parameters appropriate for acto-myosin systems. In the steady state, as we increase the active parameter  $k$  while keeping the substrate friction  $\zeta$  constant, the  $F_{\text{ext}} - v$  curve becomes non-monotonic, and two distinct regions of bistability emerge. To understand the increase of the bistability region with motor stiffness, we note that the active force is simply proportional to  $k$ , hence naively one would indeed expect its effect to be more pronounced for stiff motors. The detailed behavior is, however, determined by the interplay of the mean residence time  $\tau$  that motors spend bound to the filament and the stretch,  $\Delta$ . Soft, floppy motors have large stretches, controlled mainly by the length  $\ell_0$  traveled by an unloaded motors advancing at speed  $v_0$ . On the other hand, their residence time is small and the overall effect of the active force remains small. In contrast, stiff motors have a small stretch, of order of the stretch  $\delta_s = f_s/k$  of a stalled motor, but long residence times and are collectively capable of slowing down the filament and even holding it in place against the action of the external force, driving the negative friction instability. At even larger values of the external force motors are effectively always unbound due to the fast sliding of the filament and the velocity-force curve approaches the linear form obtained when no motors are present. This behavior is best seen from Fig. 5.

The region of non-monotonicity of the force-velocity curve and associated bistability can also be displayed as a phase diagram, as shown in Fig. 4. The stiffness of myosins is about 5 pN/nm and the actin filament friction was estimated to be of order 0.003 pNs/nm in Ref [4]. In actomyosin systems the negative friction instability should therefore be observable in a range of experimentally relevant parameters. Kinesin motors have floppier tails and a smaller stiffness of about 0.5 pN/nm. In this case bistability effects should be prevalent only at very low filament friction,  $\zeta \ll 0.001$  pNs/nm. A proper estimate of the region of parameters where the instability may be observable is rendered difficult by the fact that the onset of negative friction is also a strong function of

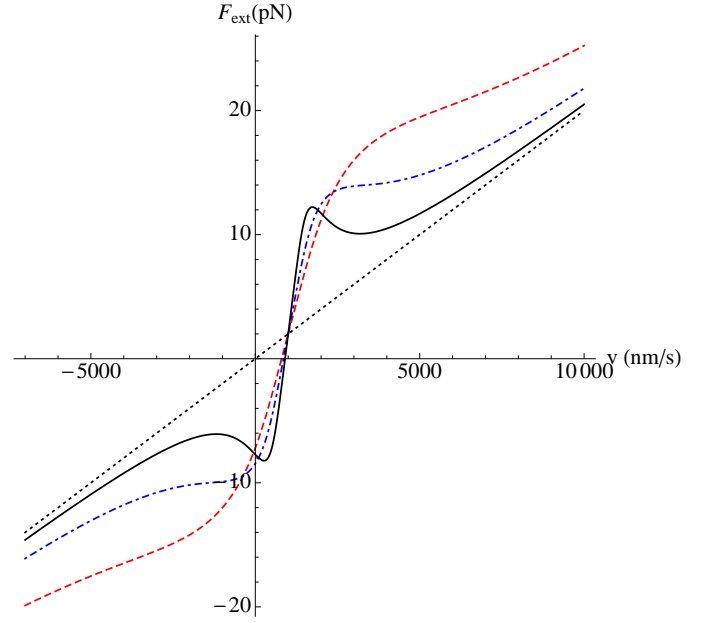


FIG. 3: (Color online) Force-velocity curves for  $\zeta = 0.002$  pNnm $^{-1}$ s and various values of the motor stiffness  $k$ , showing the transition to non-monotonicity as  $k$  increases. The values of the stiffness  $k$  (in pN/nm) and the corresponding values for  $\alpha^{-1}$  (in nm) and  $\epsilon$  are as follows:  $k = 0$ ,  $\alpha^{-1} = 0$ ,  $\epsilon = 0$  (black dotted line);  $k = 1$ ,  $\alpha^{-1} = 0.75$ ,  $\epsilon = 0.5$  (red dashed line);  $k = 2$ ,  $\alpha^{-1} = 1.5$ ,  $\epsilon = 1$  (blue dashed-dotted line);  $k = 8$ ,  $\alpha^{-1} = 6$ ,  $\epsilon = 4$  (black solid line). At high velocities the curves merge into the linear curve  $F_{\text{ext}} = \zeta v$  (black dotted line), corresponding to the case where no motors are present. The remaining parameters have the following values:  $N = \rho_m Lb = 100$ ,  $v_0 = 1000$  nm/s,  $f_s = 4$  pN,  $\omega_0 = 0.5$  (ms) $^{-1}$ ,  $r = 0.06$ .

the density of motors tethered to the substrate, which in turn affects the value of the friction  $\zeta$ . In general, we expect that a high motor density will be needed for the instability to occur. On the other hand, if the density of motors is too high, the friction  $\zeta$  will be enhanced and the instability suppressed.

We stress that the force-velocity curves displayed in Fig. 3 have been obtained by calculating  $F_{\text{ext}}$  as a function of  $v$ . In an experiment one would tune the applied force and measure the resulting velocity. The system would not access the unstable regions of negative friction, but rather follow the hysteretic path sketched in Fig. 5. The discontinuous jump may occur at the boundary of the stability region, as shown in the figure, or before such a boundary is reached, corresponding to what is known as “early switching”.

To summarize, motors have two important effects on the steady state dynamics of the filament. First, they make the filament self-propelled, in the sense that in the absence of an external force the filament will slide at a velocity  $v_s$  given by Eq. (28). The value of  $v_s$  increases with increasing motor stiffness and of course vanishes for

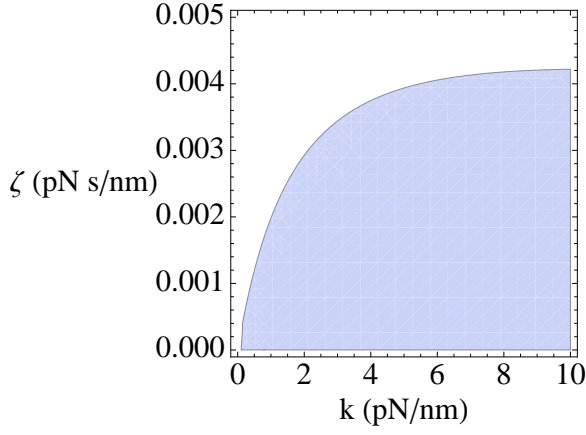


FIG. 4: (Color online) "Phase diagram" in  $k$ - $\zeta$  plane showing the region where the  $F_{\text{ext}}-v$  curves exhibit non-monotonic behavior (blue shaded region) for  $N = \rho_m Lb = 100$  and  $v_0 = 1 \mu\text{m s}^{-1}$ ,  $f_s = 4 \text{ pN}$ ,  $\alpha/k = 1.33 \text{ pN}$ ,  $\omega_0 = 0.5 \text{ (ms)}^{-1}$ ,  $r = 0.06$ .

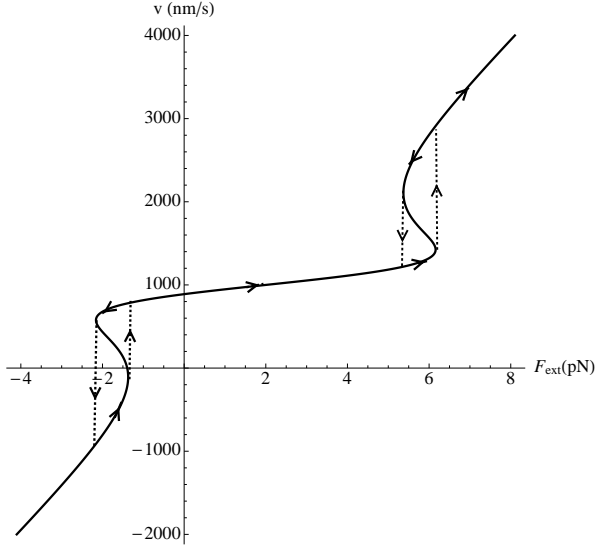


FIG. 5: The figure sketches the hysteretic behavior that may be obtained in an experiment where an external force  $F_{\text{ext}}$  is applied to a filament in a motility assay. The response of the filament will generally display two regions of hysteresis, at positive and negative forces.

$v_0 = 0$ , corresponding to the vanishing of the rate of ATP consumption  $\Delta\mu$ . The sliding velocity  $v_s$  is shown in Fig. 6 as a function of the parameter  $\epsilon$  inversely proportional to the motor stall force for a few values of the maximum number of motors that can bind to the filament. A second important effect of motor activity is the discontinuous and hysteretic response to an external force displayed in Fig. 5. When  $F_{\text{ext}} = 0$  the filament slides at the motor-induced velocity  $v_s$ . If a small force  $F_{\text{ext}} > 0$  is applied, the filament velocity remains an approximately linear function of the applied force, but with an effective

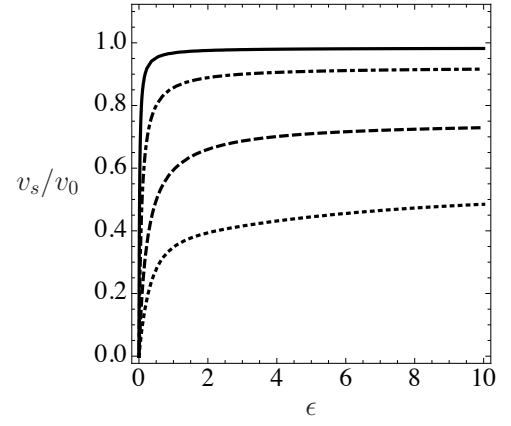


FIG. 6: The motor-induced sliding velocity  $v_s$  of an actin filament in the absence of external force is shown as a function of  $\epsilon = \ell_0/\delta_s$  for  $N = 10$  (dotted line),  $N = 25$  (dashed line),  $N = 100$  (dashed-dotted line) and  $N = 500$  (solid line). We observe that  $v_s \rightarrow v_0$  for stiff motors as  $N$  is increased. Parameter values:  $\zeta = 0.002 \text{ pN (nm)}^{-1}\text{s}$ ,  $r = 0.06$ ,  $\alpha/k = 1.33 \text{ pN}$ .

friction greatly enhanced by motor binding/unbinding. This enhancement of friction is also termed in the literature as protein friction [28]. At high velocity, only a few motors are attached to the filament and the filament velocity approaches the value it would have in the absence of motors as the applied force is increased beyond a characteristic value. When the external force is ramped down the filament velocity jumps to the lower branch corresponding to a lower value of the force, resulting in hysteresis.

## B. Fluctuation Dynamics

We now examine the dynamics of noise-induced fluctuations about the steady state by letting  $\delta\dot{x} = \dot{x} - v$ , where  $v$  is the steady state velocity, given by the solution of Eq. (23) discussed in the previous section. The dynamics of the fluctuation  $\delta\dot{x}$  is then described by the equation

$$\zeta\delta\dot{x} = -kN\Delta(v)\delta p_b - kNp_{bs}\delta\Delta + \eta(t), \quad (30)$$

where both  $\delta\Delta = [\partial_v\Delta(v)]\delta\dot{x}$  and  $\delta p_b(t)$  depend on noise only implicitly through the velocity  $\dot{x}$ , with

$$\partial_t\delta p_b = -\left[\frac{1}{\tau(v)} + \omega_b\right]\delta p_b - p_{bs}(v)\frac{\partial}{\partial v}\left[\frac{1}{\tau(v)}\right]\delta\dot{x} \quad (31)$$

The random force  $\eta(t)$  in Eq. (30) describes noise on the filament, with  $\langle\eta(t)\rangle = 0$  and  $\langle\eta(t)\eta(t')\rangle = 2B\delta(t-t')$ . Noise can arise in the system from a variety of sources, including the fluid through which the filament moves and the motor on/off dynamics. For simplicity we assume the spectrum is white, albeit with a non-thermal strength  $B$ .



By solving Eq. (31) with initial condition  $\delta p_b(t=0) = 0$  and substituting in Eq. (30), we obtain a single equation for  $\delta \dot{x}$ ,

$$[\zeta + \zeta_a(v)] \delta \dot{x}(t) + \omega_0 \zeta'_a(v) \int_0^t dt' e^{-\Omega(t-t')} \delta \dot{x}(t') = \eta(t) \quad (32)$$

where we have introduced an effective frequency  $\Omega(v) = \tau^{-1}(v) + \omega_b$  and active frictions

$$\zeta_a(v) = kNp_{bs}(v)\partial_v \Delta(v) \quad (33)$$

$$\zeta'_a(v) = kNp_{bs}(v)\Delta(v) \frac{\partial}{\partial v} \left( \frac{1}{\tilde{\tau}} \right). \quad (34)$$

In all the parameters defined above  $v$  has to be replaced by the steady state solution obtained in the previous sec-

tion. The time scale  $\Omega^{-1}$  represent the duration of the cycle of a loaded motor. Note that  $\zeta_a(v=0) = \zeta_a$ , with  $\zeta_a$  given by Eq. (27). It is evident from Eq. (32) that motor dynamics yields a non-Markovian contribution to the friction.

If we neglect the load dependence of the unbinding rate by letting  $\nu = 0$ , hence  $\tau^{-1} = \omega_0$ , then  $\zeta_a(v) = \zeta_{a0} = Nrkl/v_0$  and  $\zeta'_a(v) = 0$ . In this limit  $\langle [\delta x(t) - \delta x(0)]^2 \rangle = 2D_{a0}t$  and is diffusive *at all times*, with an effective diffusion constant  $D_{a0} = \frac{B}{(\zeta + \zeta_{a0})^2}$ .

When  $\nu$  is finite we obtain

$$\langle [\delta x(t) - \delta x(0)]^2 \rangle = 2D_a t + 4D_a \left[ \frac{\zeta'_a(v)\omega_0}{[\zeta + \zeta_a(v)]\Omega_a} \right]^2 \left( t - \frac{1 - e^{-\Omega_a t}}{\Omega_a} \right), \quad (35)$$

where  $D_a = B/[\zeta + \zeta_a(v)]^2$  and  $\Omega_a(v) = \Omega(v) + \omega_0 \zeta'_a(v)/[\zeta + \zeta_a(v)]$ . The characteristic time scale  $\Omega_a^{-1}$  controls the crossover from ballistic behavior for  $t \ll \Omega_a^{-1}$  to diffusive behavior for  $t \gg \Omega_a^{-1}$ . It is determined by the smaller of two time scales:  $\Omega^{-1}$ , defined after Eq. (32), that represents the duration of the cycle of a loaded motor, and the active time  $(\omega_0 \zeta'_a/[\zeta + \zeta_a])^{-1}$  that represents the correlation time for the effect of motor on/off dynamics on the filament. At long times the mean-square displacement is always diffusive, with an effective diffusion constant

$$D_{\text{eff}} = D_a \left[ 1 + \left( \frac{\zeta'_a \omega_0}{[\zeta + \zeta_a(v)]\Omega_a} \right)^2 \right] \quad (36)$$

This result only describes the behavior of the system in the stable region, where the effective friction remains positive. At the onset of negative friction instability  $\zeta + \zeta_a(v) \rightarrow 0$  and the effective diffusivity diverges. In other words the instability is also associated with large fluctuations in the rod's displacements due to the cooperative motor dynamics.

To leading order in  $\nu$  the frequency  $\Omega_a$  that controls the crossover to diffusive behavior is simply  $\Omega \simeq \omega_0 + \omega_b + \mathcal{O}(\nu^2)$ . For non-processive motors such as myosins  $\omega_0 \gg \omega_b$  and  $\Omega \sim \omega_0$ . The effective diffusion constant is given by

$$D_{\text{eff}} \simeq D_a \left[ 1 + \frac{2\zeta^2 \zeta_{a0}}{(\zeta + \zeta_{a0})^3} \left( \frac{v_0 \alpha}{\omega_0(1 + \epsilon)} \right)^2 + [(v_0 \alpha / \omega)^4] \right]. \quad (37)$$

This expression indicates that the enhancement of the diffusion constant comes from the competition of the

ballistic motor-driven motion of the filament at speed  $\sim v_0 \zeta_{a0}/(\zeta + \zeta_{a0})$  and the randomization of such motion by the motor on/off dynamics on time scales  $\sim \omega_0^{-1}$ . The result is that the filament dynamics is diffusive at long times, but with an enhanced diffusion constant.

Finally, we stress that the correlation function  $\langle [\delta x(t) - \delta x(0)]^2 \rangle$  describes the fluctuations about the steady state value  $vt$ . If we write  $x(t) = vt + \delta x(t)$  the actual mean square displacement of the center of mass of the rod is given by  $\langle (x(t) - x(0))^2 \rangle = v^2 t^2 + \langle [\delta x(t) - \delta x(0)]^2 \rangle$  and is ballistic at long times in one dimension due to the mean motion of the rod. In addition, due to nonlinearity of the Langevin equation (17) the mean value  $\langle x \rangle$  in the presence of noise will in general differ from the steady state solution  $vt$  obtained in the absence of noise due to renormalization by fluctuations  $\langle F_a(\dot{x}, t) \rangle - F_a(v, t)$ . These fluctuations are neglected in mean field theory.

#### IV. ACTIVE FILAMENT DYNAMICS IN TWO DIMENSIONS

In two dimensions the coupled translational and rotational dynamics of the filament is described by Eqs. (1a) and (1b). It is convenient to write the instantaneous velocity of the center of the filament in terms of components longitudinal and transverse to the long axis of the filament,  $\dot{\mathbf{r}} = V_{\parallel} \hat{\mathbf{u}} + V_{\perp} \hat{\mathbf{n}}$ . Similarly the stretch is written as  $\Delta = \Delta_{\parallel} \hat{\mathbf{u}} + \Delta_{\perp} \hat{\mathbf{n}}$ , where (see Eq. (12b))

$$\Delta_{\parallel} = \hat{\mathbf{u}} \cdot \Delta = (V_{\parallel} + v_m) \tau, \quad (38a)$$

$$\Delta_{\perp} = \hat{\mathbf{n}} \cdot \Delta = (V_{\perp} + s_0 \dot{\theta}) \tau. \quad (38b)$$

It is then clear that  $\Delta_{\parallel}$  has the same form as in one dimension

$$\Delta_{\parallel} = \frac{(V_{\parallel} - v_0)/\omega_0}{\tilde{\tau}^{-1} + \epsilon}, \quad (39)$$

and the mean-field value of the attachment time  $\tau$  is given by

$$\tilde{\tau}^{-1}(V_{\parallel}, V_{\perp}, \dot{\theta}) = 1 + \frac{(V_{\parallel} - v_0)^2 \alpha^2}{(\tilde{\tau}^{-1} + \epsilon)^2 \omega_0^2} + \frac{V_{\perp}^2 \tilde{\tau}^2 \alpha^2}{\omega_0^2} + \frac{L^2 \dot{\theta}^2 \tilde{\tau}^2 \alpha^2}{12 \omega_0^2}, \quad (40)$$

where we have carried out the average over  $s_0$ . Inserting these expressions in Eqs. (15) and (16), the mean field active force and torque exerted by bound motors on the filament can then be written as

$$\mathbf{F}_a = -kNp_b(t) \left[ \frac{(V_{\parallel} - v_0)/\omega_0}{\tilde{\tau}^{-1} + \epsilon} \hat{\mathbf{u}} + V_{\perp} \tau \hat{\mathbf{n}} \right], \quad (41a)$$

$$T_a = -kNp_b(t)\tau \left[ \frac{L^2 \dot{\theta}}{12} + V_{\perp} v_m \tau \right]. \quad (41b)$$

### A. Steady State and its stability

The steady state of the motor-driven filament in two dimensions in the absence of noise is characterized by the center of mass velocity  $\mathbf{v} = v_{\parallel} \hat{\mathbf{u}} + v_{\perp} \hat{\mathbf{n}}$  and angular velocity  $\dot{\theta}$ . In the absence of any external force or torque,  $\dot{\theta}$  and  $v_{\perp}$  are identically zero, whereas the longitudinal dynamics described by  $v_{\parallel}$  is identical to that obtained in one-dimension: the filament will slide along its long axis at a steady longitudinal velocity  $v_{\parallel} = F_p/(\zeta + \zeta_a)$ , with  $F_p$  and  $\zeta_a$  given by Eqs. (26) and (27), respectively.

To gain some insight into the stability of the system under application of external forces or torques, we expand  $\mathbf{F}_a$  and  $T_a$  to linear order in velocities  $\mathbf{v}$  and  $\dot{\theta}$  as,  $\mathbf{F}_a(\mathbf{v}, \dot{\theta}) \simeq \mathbf{F}_p + \left( \frac{\partial \mathbf{F}_a}{\partial v_{\parallel}} \right)_0 v_{\parallel} + \left( \frac{\partial \mathbf{F}_a}{\partial v_{\perp}} \right)_0 v_{\perp} + \left( \frac{\partial \mathbf{F}_a}{\partial \dot{\theta}} \right)_0 \dot{\theta}$ , and  $T_a(\mathbf{v}, \dot{\theta}) \simeq \left( \frac{\partial T_a}{\partial v_{\parallel}} \right)_0 v_{\parallel} + \left( \frac{\partial T_a}{\partial v_{\perp}} \right)_0 v_{\perp} + \left( \frac{\partial T_a}{\partial \dot{\theta}} \right)_0 \dot{\theta}$ , where  $\mathbf{F}_p = \mathbf{F}_{a,0} = F_p \hat{\mathbf{u}}$ , is the tangential propulsion force due to the motors. The subscript ‘0’ indicates that the expressions are evaluated at  $\mathbf{v} = 0$  and  $\dot{\theta} = 0$ . This leads to steady state force/velocity and torque/velocity relations of the form

$$\left( \underline{\zeta} + \underline{\zeta}_a \right) \cdot \mathbf{v} = \mathbf{F}_{\text{ext}} + F_p \hat{\mathbf{u}}, \quad (42a)$$

$$(\zeta_{\theta} + \zeta_{\theta a}) \dot{\theta} = T_{\text{ext}} - g_a v_{\perp}, \quad (42b)$$

where we have introduced an active “momentum”  $g_a$  given by  $g_a = -\left( \frac{\partial T_a}{\partial v_{\perp}} \right)_0$ . The active contributions to the longitudinal, transverse and rotational friction coefficients are defined as  $\zeta_{\parallel a} = -\hat{\mathbf{u}} \cdot \left( \frac{\partial \mathbf{F}_a}{\partial v_{\parallel}} \right)_0$ ,  $\zeta_{\perp a} = -\hat{\mathbf{n}} \cdot \left( \frac{\partial \mathbf{F}_a}{\partial v_{\perp}} \right)_0$ , and  $\zeta_{\theta a} = -\left( \frac{\partial T_a}{\partial \dot{\theta}} \right)_0$ . The longitudinal friction coefficient  $\zeta_{\parallel a}$  is identical to the active friction

$\zeta_a$  given in Eq. (27) for a rod in one dimension, with  $\Delta \rightarrow \Delta_{\parallel}$ . The transverse and rotational friction coefficients are enhanced by motor activity. Their active components are given by

$$\zeta_{\perp a} = \frac{kNr\tau_0}{r + (1-r)\tilde{\tau}_0^{-1}} \quad (43a)$$

$$\zeta_{\theta a} = \frac{kNr\tau_0 L^2/12}{r + (1-r)\tilde{\tau}_0^{-1}}. \quad (43b)$$

Finally we have,  $g_a = \frac{kNr\tau_0 v_0 (\tau_0 + \epsilon |\Delta_{\parallel}^0|)}{r + (1-r)\tilde{\tau}_0^{-1}}$ . When the load dependence of the unbinding rate is neglected ( $\nu = 0$ ), all friction coefficients are enhanced by motor activity. When the force/velocity and torque/angular velocity curves are calculated to nonlinear order, we find that the only instability is the negative longitudinal friction instability obtained in one dimension. No instabilities are obtained in the angular dynamics. We expect this will change if we include the semiflexibility of the filament [29, 30].

### B. Fluctuations around the steady state

We now examine the dynamics of noise-induced fluctuations about the steady state by letting  $\delta \dot{\mathbf{r}} = \dot{\mathbf{r}} - \mathbf{v}$  and  $\delta \dot{\theta} = \dot{\theta} - \dot{\theta}$  where  $\mathbf{v}$  and  $\dot{\theta}$  are the steady state velocity and angular frequency in the absence of external force and torque. As noted in the previous section when  $\mathbf{F}_{\text{ext}} = 0$  and  $T_{\text{ext}} = 0$ ,  $v_{\parallel} = v \neq 0$ , with  $v$  given by the solution of Eq. (23), and  $v_{\perp} = \dot{\theta} = 0$ . Projecting velocity fluctuations longitudinal and transverse to the filament,  $\delta \dot{\mathbf{r}} = \hat{\mathbf{u}} \delta V_{\parallel} + \hat{\mathbf{n}} \delta V_{\perp}$ , the dynamics of fluctuations is described by the coupled equations,

$$[\zeta_{\parallel} + \zeta_{\parallel a}(v)] \delta V_{\parallel} = -kN\Delta_{\parallel}(v) \delta p_b(t) + \eta_{\parallel}, \quad (44a)$$

$$[\zeta_{\perp} + \zeta_{\perp a}(v)] \delta V_{\perp} = \eta_{\perp}, \quad (44b)$$

$$[\zeta_{\theta} + \zeta_{\theta a}(v)] \delta \dot{\theta} = -kNp_{bs}(v)\tau(v)v_m(v)\delta V_{\perp} + \eta_{\theta}, \quad (44c)$$

with

$$[\zeta_{\theta} + \zeta_{\theta a}(v)] \delta \dot{p}_b = -\Omega(v) \delta p_b - p_{bs}(v) \frac{\partial}{\partial v} \left[ \frac{1}{\tau(v)} \right] \delta V_{\parallel}, \quad (45)$$

where the effective frequency  $\Omega(v) = \tau^{-1}(v) + \omega_b$  and the longitudinal active friction  $\zeta_{\parallel a}(v)$  are as in one dimension,  $\zeta_{\perp a}(v) = kNp_{bs}(v)\tau(v)$  and  $\zeta_{\theta a}(v) = kNp_{bs}(v)\tau(v)L^2/12$ . In all the parameters,  $v \equiv v_{\parallel}$  has to be replaced by the steady state solution obtained in one dimension in the absence of external force or torque.

The time-correlation function of orientational fluctuations,  $\Delta\theta(t) = \delta\theta(t) - \delta\theta(0)$ , can be calculated from Eqs. (44b) and (44c), with the result

$$\langle \Delta\theta(t) \Delta\theta(t') \rangle = 2D_{\theta a} \min(t, t'). \quad (46)$$

The effective rotational diffusion constant is enhanced by the transverse diffusivity and is given by

$$D_{\theta a}(v) = \frac{B_{\theta}}{[\zeta_{\theta} + \zeta_{\theta a}(v)]^2} + \frac{B_{\perp}/\ell_p^2(v)}{[\zeta_{\perp} + \zeta_{\perp a}(v)]^2} \quad (47)$$

with  $\ell_p(v) = [\zeta_{\theta} + \zeta_{\theta a}(v)]/kNp_{bs}(v)\tau(v)v_m(v)$ . Using Eq. (46), one immediately obtains the angular time-correlation function as [31],

$$\langle \hat{\mathbf{u}}(t') \cdot \hat{\mathbf{u}}(t'') \rangle = e^{-D_{\theta a}|t'-t''|}. \quad (48)$$

The fluctuations in the probability of bound motors are driven by their coupling to the stochastic longitudinal dynamics of the filament. Assuming  $\delta p_b(0) = 0$ , we obtain

$$\langle \delta p_b(t) \delta p_b(t') \rangle = \left( \frac{\zeta'_a \omega_0}{v_p} \right)^2 \frac{B_{\parallel}}{\Omega_a} \left[ e^{-\Omega_a|t-t'|} - e^{-\Omega_a(t+t')} \right], \quad (49)$$

where  $\Omega_a(v) = \Omega(v) + \omega_0 \frac{\zeta'_a(v)}{\zeta_{\parallel} + \zeta_{\parallel a}(v)}$ ,  $\zeta'_a(v) = kNp_{bs}(v)\Delta_{\parallel}(v)\frac{\partial}{\partial v}(\frac{1}{\tau})$ , and  $v_p(v) = Nk\Delta_{\parallel}(v)/[\zeta_{\parallel} + \zeta_{\parallel a}(v)]$  is a longitudinal propulsion velocity. Notice that  $v_p(v=0) = v_s/p_{bs0}$ , with  $v_s$  given in Eq. (28). Finally, we can compute the correlation function of the fluctuation  $\delta \mathbf{r}$  of the filament's position. In the laboratory frame the dynamics of  $\delta \mathbf{r}$  can be recast in the form of a simple equation,

$$\delta \dot{\mathbf{r}} = -v_p \delta p_b(t) \hat{\mathbf{u}} + \left[ \underline{\zeta} + \underline{\zeta}^a(v) \right]^{-1} \cdot \boldsymbol{\eta} \quad (50)$$

Fluctuations in the probability of bound motors do not couple to orientational fluctuations to linear order. It is then straightforward to calculate the correlation function of displacement fluctuations, with the result

$$\langle [\delta \mathbf{r}(t) - \delta \mathbf{r}(0)]^2 \rangle = 2D_{\text{eff}} t + \frac{D_{\parallel a} \zeta_a'^2 \omega_0^2 / \Omega_a^2}{(D_{\theta a}^2 - \Omega_a^2)(\zeta_{\parallel} + \zeta_{\parallel a})^2} \left[ -(D_{\theta a} + \Omega_a)(1 - e^{-2\Omega_a t}) + \frac{4\Omega_a^2}{D_{\theta a} + \Omega_a} (1 - e^{-(\Omega_a + D_{\theta a})t}) \right] \quad (51)$$

where effective longitudinal and transverse diffusion constants have been defined as

$$D_{\parallel a} = B_{\parallel}/[\zeta_{\parallel} + \zeta_{\parallel a}(v)]^2, \quad (52a)$$

$$D_{\perp a} = B_{\perp}/[\zeta_{\perp} + \zeta_{\perp a}(v)]^2. \quad (52b)$$

Finally, using  $\mathbf{r}(t) = \delta \mathbf{r}(t) + \int_0^t dt' v \hat{\mathbf{u}}(t')$ , the mean square displacement (MSD) can be written as,

$$\langle [\mathbf{r}(t) - \mathbf{r}(0)]^2 \rangle = \langle [\delta \mathbf{r}(t) - \delta \mathbf{r}(0)]^2 \rangle + \frac{v^2}{D_{\theta a}} \left[ t - \frac{1 - e^{-D_{\theta a} t}}{D_{\theta a}} \right]. \quad (53)$$

The MSD is controlled by the interplay of two time scales, the rotational diffusion time,  $D_{\theta a}^{-1}$ , that is decreased by activity as compared to its bare value,  $D_{\theta}^{-1}$ , and the time scale  $\Omega_a^{-1}$ , which is turn controlled by the duration of the motor binding/unbinding cycle. If  $D_{\theta a}^{-1} \gg \Omega_a^{-1}$ , which is indeed the case for actomyosin systems [35] then on times  $t \gg \Omega_a^{-1}$  the MSD is given by

$$\langle [\mathbf{r}(t) - \mathbf{r}(0)]^2 \rangle = 2D_{\text{eff}} t + \frac{v^2}{D_{\theta a}} \left[ t - \frac{1 - e^{-D_{\theta a} t}}{D_{\theta a}} \right], \quad (54)$$

with

$$D_{\text{eff}} = D_{\parallel a} + D_{\perp a} + \frac{D_{\parallel a} \Omega_a}{D_{\theta a} + \Omega_a} \left( \frac{\zeta'_a \omega_0}{[\zeta_{\parallel} + \zeta_{\parallel a}(v)] \Omega_a} \right)^2. \quad (55)$$

In other words the rod performs a persistent random walk consisting of ballistic segments at speed  $v$  randomized

by rotational diffusion. The behavior is diffusive both at short and long times, albeit with different diffusion constants,  $D_{\text{eff}}$  and  $D_{\text{eff}} + v^2/(2D_{\theta a})$ , respectively. This is indeed the dynamics of a self-propelled rod. If the noise strengths  $B_{\parallel}$ ,  $B_{\perp}$  and  $B_{\theta}$  are negligible, then Eq. (54) reduces to

$$\langle [\mathbf{r}(t) - \mathbf{r}(0)]^2 \rangle \simeq \frac{v^2}{D_{\theta a}} \left[ t - \frac{1 - e^{-D_{\theta a} t}}{D_{\theta a}} \right]. \quad (56)$$

and the MSD exhibits a crossover from ballistic behavior for  $t \ll D_{\theta a}^{-1}$  to diffusive at long times.

It is worthwhile to note that if one neglects load dependence of unbinding rate by taking  $\nu = 0$ , effective diffusivity at long time is enhanced with,  $D_{\text{eff}}^0 = D_{\parallel a}^0 + D_{\perp a}^0 + (v^0)^2/2D_{\theta a}^0$ , due to the interplay between ballistic motion driven by the tethered motors and rotational diffusion, unlike the situation in one dimension.

## V. SUMMARY AND OUTLOOK

We have investigated the dynamics of a single cytoskeletal filament modeled as a rigid rod interacting with tethered motor proteins in a motility assay in two dimensions. Motor activity yields both an effective propulsion of the filament along its long axis and a renormalization of all friction coefficients. The longitudinal friction can

change sign leading to an instability in the filament's response to external force, as demonstrated by previous authors [11]. The effective propulsion force and filament velocity in the steady state are calculated in terms of microscopic motor and filament parameters.

We also considered the fluctuations of the filament displacement about its steady state value and demonstrated that the coupling to the binding/unbinding dynamics of the the motors yields non-Markovian fluctuations and enhanced diffusion. Future work will include the stochasticity in the motor displacements and the semiflexibility of filaments, which is expected to lead to buckling instabilities [32] and anomalous fluctuations [33].

### Acknowledgments

This work was supported at Syracuse by the National Science Foundation under a Materials World Network award DMR-0806511 and in Stellenbosch by the National Research Foundation under grant number UID 67512. MCM was also partly supported on NSF-DMR-1004789 and NSF-DMR-0705105. We thank Aparna Baskaran, Lee Boonzaaier and Tannie Liverpool for illuminating discussions. Finally, SB and MCM thank the University of Stellenbosch for hospitality during the completion of part of this work.

### Appendix A: Solution of Mean-Field Equation

Here we discuss the solution of the mean-field equation (13) for the attachment time  $\tau$ . For simplicity, we consider the one-dimensional case in detail. The discussion is then easily generalized to two dimensions. The mean-field equation for the residence time  $\tau$  is rewritten here for clarity:

$$\tau_{MF} = \omega_u^{-1}(\Delta(\tau_{MF})). \quad (\text{A1})$$

The solution clearly depends on the form chosen to describe the dependence of the motor unbinding rate on the stretch  $\Delta$ , in turn given by  $\Delta(\tau_{MF}) = (\dot{x} - v_0)/(\tau_{MF}^{-1} + \epsilon\omega_0)$ . The mean-field equation must be inverted to determine  $\tau_{MF}$  as a function of the filament velocity  $\dot{x} = v$ . For compactness we drop the label 'MF'. It is clear that  $\tau$  has a maximum at  $v = v_0$ , where  $\tau = \omega_0^{-1}$ . This simply corresponds to the fact that the time a motor protein spends attached to the actin filament is largest when the motors' tails are unstretched ( $\Delta = 0$ ) and the motors advance at the unloaded motor velocity,  $v_0$ .

It is convenient to use the dimensionless variable and parameters introduced in the text and write the stretch  $\Delta$  as

$$\Delta = \frac{(u - 1)\ell_0}{\tilde{\omega}_u + 1}, \quad (\text{A2})$$

where  $u = v/v_0$ ,  $\tilde{\omega}_u = \omega_u/\omega_0$  and  $\ell_0 = v_0/\omega_0$ . A form commonly used in the literature is the exponential form

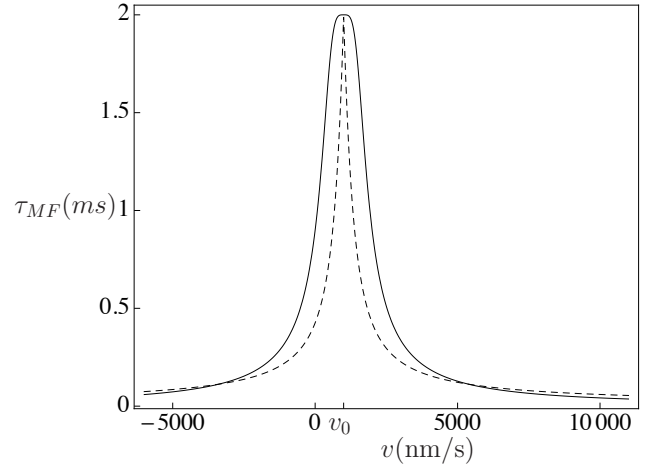


FIG. 7: Mean field attachment time  $\tau_{MF}$  as a function of  $v$  for parameter values appropriate for acto-myosin systems:  $v_0 = 1000 \text{ nm s}^{-1}$ ,  $k = 10 \text{ pN nm}^{-1}$ ,  $f_s = 4 \text{ pN}$ ,  $\alpha^{-1} = 7.5 \text{ nm}$ ,  $\omega_0 = 0.5 \text{ (ms)}^{-1}$ ,  $r = 0.06$ , corresponding to  $\epsilon = 5$ . The dashed line is the numerical solution of Eq. (A1) obtained using the exponential dependence of the unbinding rate on the stretch. The solid line is obtained using the parabolic ansatz given in Eq. (A3).

$\omega_u(\Delta) = \omega_0 e^{\alpha|\Delta|}$ , with  $\alpha^{-1}$  a characteristic length scale. The dimensionless combination  $\alpha\Delta$  can then be written in terms of the parameter  $\nu = \alpha\ell_0/(1 + \epsilon)$  and setting  $\nu = 0$  corresponds to neglecting the load dependence of the unbinding rate. The numerical solution of Eq. (A1) for the mean attachment time as a function of  $v$  is shown as a dashed line in Fig. 7 for parameter values appropriate for acto-myosin systems. As expected it has a sharp maximum at  $v = v_0$ . At large  $v$  the attachment time decays logarithmically with velocity. As a result, the stretch is found to saturate at large velocity, as shown by the dashed curve in Fig. 8. This behavior is unphysical as it does not incorporate the fact that when the stretch exceeds a characteristic value of the order  $f_d/k$ , the motor head simply detaches, as shown in Fig. 2. Instead of incorporating this cutoff by hand, we have chosen to use a simple quadratic form for the dependence of the unbinding rate on the stretch, given by

$$\omega_u(\Delta) = \omega_0 [1 + \alpha^2 \Delta^2]. \quad (\text{A3})$$

With this form the mean field equation (A1) can be solved analytically, although the explicit solution is not terribly informative and will not be given here. The resulting attachment time is shown as a solid line in Fig. 7. The quadratic form reproduces the sharp maximum of  $\tau$  at  $v = v_0$  and yields  $\tau \sim v^{-3/2}$  at large  $v$ . The stretch then decays with velocity, as shown in Fig. 8.

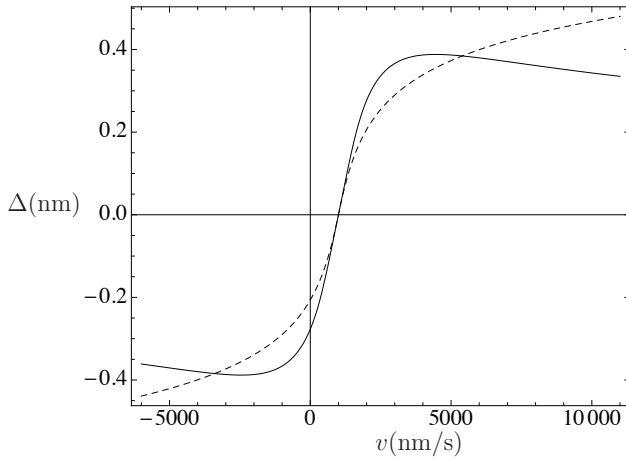


FIG. 8: Stretch  $\Delta$  as a function of velocity  $v$  obtained using the mean-field value of the attachment time displayed in Fig. 7. The parameter values are the same as in Fig. 7. The dashed line is obtained using the exponential dependence of the unbinding rate on the stretch. The solid line is obtained using the parabolic ansatz given in Eq. (A3).

- 
- [1] V. Schaller, C. Weber, C. Semmrich, E. Frey, and A. R. Bausch, *Nature* **467**, 73 (2010).
  - [2] T. Butt, T. Mufti, A. Humayun, P. B. Rosenthal, S. Khan, S. Khan, and J. E. Molloy, *J. Biol. Chem.* **285**, 4964 (2010).
  - [3] M. F. Copeland and D. B. Weibel, *Soft Matter* **5**, 1174 (2009).
  - [4] D. Riveline, A. Ott, F. Jülicher, D. A. Winkelmann, O. Cardoso, J.-J. Lacapère, S. Magnúsdóttir, J. L. Viovy, L. Gorre-Talini, and J. Prost, *Eur. Biophys. J.* **27**, 403 (1998).
  - [5] T. Guérin, J. Prost, P. Martin, and J.-F. Joanny, *Curr. Op. Cell Biol.* **22**, 14 (2010).
  - [6] F. Jülicher and J. Prost, *Phys. Rev. Lett.* **78**, 4510 (1997), URL <http://link.aps.org/doi/10.1103/PhysRevLett.78.4510>.
  - [7] S. W. Grill, K. Kruse, and F. Jülicher, *Phys. Rev. Lett.* **94**, 108104 (2005), URL <http://dx.doi.org/10.1103/PhysRevLett.94.108104>.
  - [8] S. Günther and K. Kruse, *New J. Phys.* **9**, 417 (2007), URL <http://iopscience.iop.org/1367-2630/9/11/417/>.
  - [9] A. Vilfan and E. Frey, *Journal of Physics: Condensed Matter* **17**, S3901 (2005), URL <http://stacks.iop.org/0953-8984/17/i=47/a=018>.
  - [10] S. Camalet and F. Jülicher, *New Journal of Physics* **2**, 24 (2000), URL <http://stacks.iop.org/1367-2630/2/i=1/a=324>.
  - [11] F. Jülicher and J. Prost, *Phys. Rev. Lett.* **75**, 2618 (1995), URL <http://link.aps.org/doi/10.1103/PhysRevLett.75.2618>.
  - [12] M. Badoual, F. Jülicher, and J. Prost, *Proc. Natl. Acad. Sci. USA* **99**, 6696 (2002).
  - [13] P. Y. Plaçais, M. Balland, T. Guérin, J.-F. Joanny, and P. Martin, *Phys. Rev. Lett.* **103**, 158102 (2009), URL <http://link.aps.org/doi/10.1103/PhysRevLett.103.158102>.
  - [14] F. Gibbons, J. F. Chauwin, M. Despósito, and J. V. José, *Biophys. J.* **80**, 2515 (2001).
  - [15] P. Kraikivski, R. Lipowsky, and J. Kierfeld, *Phys. Rev. Lett.* **96**, 258103 (2006), URL <http://link.aps.org/doi/10.1103/PhysRevLett.96.258103>.
  - [16] C. J. Brokaw, *Proc. Natl. Acad. Sci. USA* **72**, 3102 (1975).
  - [17] A. Vilfan, E. Frey, and F. Schwabl, *Europhys. Lett.* **283**, 45 (1999).
  - [18] D. Hexner and Y. Kafri, *Phys Biol* **6**, 036016 (2009), URL <http://iopscience.iop.org/1478-3975/6/3/036016>.
  - [19] T. Guérin, J. Prost, and J.-F. Joanny, *Phys. Rev. Lett.* **104**, 248102 (2010), URL <http://prl.aps.org/abstract/PRL/v104/i24/e248102>.
  - [20] A. F. Huxley, *Prog. Biophys. Chem.* **7**, 255 (1957).
  - [21] A. Vilfan, *Biophys. J.* **113**, 2515 (2009).
  - [22] S. van Teeffelen and H. Löwen, *Phys. Rev. E* **78**, 020101 (2008), URL <http://pre.aps.org/abstract/PRE/v78/i2/e020101>.
  - [23] A. Baskaran and M. C. Marchetti, *Phys. Rev. Lett.* **101**, 268101 (2008).
  - [24] K. Svoboda and S. M. Block, *Cell* **77**, 773 (1994).
  - [25] A. Parmeggiani, F. Jülicher, L. Peliti, and J. Prost, *Europhys. Lett.* **56**, 603 (2001), cond-mat/0109187v1, URL <http://arxiv.org/abs/cond-mat/0109187v1>.
  - [26] K. Visscher, M. J. Schnitzer, and S. M. Block, *Nature* **400**, 184 (1999), URL <http://www.nature.com/nature/journal/v400/n6740/abs/400184a0.html>.
  - [27] J. Howard, *Mechanics of Motor Proteins and the Cytoskeleton* (Sinauer Associates, 2001), ISBN 0878933344, URL <http://www.amazon.com/exec/obidos/redirect?>

- tag=citeulike07-20&path=ASIN/0878933344.
- [28] K. Tawada and K. Sekimoto, Journal of Theoretical Biology **150**, 193 (1991), ISSN 0022-5193, URL <http://www.sciencedirect.com/science/article/B6WMD-4KDGR4D-5/2/906e9dbabbba82beff6bc6e5f982d9bd>.
  - [29] N. Kikuchi, A. Ehrlicher, D. Koch, J. A. Käs, S. Ramaswamy, and M. Rao, Proceedings of the National Academy of Sciences **106**, 19776 (2009).
  - [30] C. P. Brangwynne, G. H. Koenderink, F. C. MacKintosh, and D. A. Weitz, Phys. Rev. Lett. **100**, 118104 (2008).
  - [31] Y. Han, A. Alsayed, M. Nobili, J. Zhang, T. C. Lubensky, and A. G. Yodh, Science **314**, 626 (2006), URL <http://www.sciencemag.org/content/314/5799/626.short>.
  - [32] D. Karpeev, I. S. Aranson, L. S. Tsimring, and H. G. Kaper, Phys. Rev. E **76**, 051905 (2007).
  - [33] T. B. Liverpool, Phys. Rev. E **67**, 031909 (2003), URL <http://pre.aps.org/abstract/PRE/v67/i3/e031909>.
  - [34]  $\alpha$  can be estimated to be equal to  $ka/k_B T$ , where  $a$  is a microscopic length scale of the order of a few nm. Experiments are carried out at room temperatures which leads to  $k_B T \sim pNnm$ .
  - [35] A naive estimate for actin-myosin systems (neglecting the load dependence of the unbinding rate) gives  $\Omega_a^0 \simeq 5 \text{ ms}^{-1}$  and  $D_{\theta a}^0 \simeq 0.17 \text{ s}^{-1}$  for  $N = 1$ .